 Human Molecular Genetics, 2002, Vol. 11, No. 23 2837–2844

# Charcot–Marie–Tooth disease neurofilament mutations disrupt neurofilament assembly and axonal transport

**Janet Brownlees, Steven Ackerley, Andrew J. Grierson†, Nick J.O. Jacobsen, Kerry Shea, Brian H. Anderton, P. Nigel Leigh, Christopher E. Shaw and Christopher C.J. Miller***

Department of Neuroscience and Department of Neurology, The Institute of Psychiatry, King's College London, De Crespigny Park, Denmark Hill, London SE5 8AF, UK

Received June 20, 2002; Revised and Accepted August 20, 2002

**Charcot–Marie–Tooth disease (CMT) is the most common inherited disorder of the peripheral nervous system, and mutations in neurofilaments have been linked to some forms of CMT. Neurofilaments are the major intermediate filaments of neurones, but the mechanisms by which the CMT mutations induce disease are not known. Here, we demonstrate that CMT mutant neurofilaments disrupt both neurofilament assembly and axonal transport of neurofilaments in cultured mammalian cells and neurones. We also show that CMT mutant neurofilaments perturb the localization of mitochondria in neurones. Accumulations of neurofilaments are a pathological feature of several neurodegenerative diseases, including amyotrophic lateral sclerosis (ALS), Alzheimer's disease, Parkinson's disease, dementia with Lewy bodies, and diabetic neuropathy. Our results demonstrate that aberrant neurofilament assembly and transport can induce neurological disease, and further implicate defective neurofilament metabolism in the pathogenesis of human neurodegenerative diseases.**

## INTRODUCTION

Charcot–Marie–Tooth disease (CMT) is a group of neuropathies that constitute the most common inherited disorders of the peripheral nervous system (1). Mutations in a number of genes cause CMT (2–6), and mutations in neurofilament light chain have recently been demonstrated to cause a form of type- 2 CMT (7,8).

Neurofilaments are the major intermediate filaments of neurones and in most mature neurones contain three subunit proteins: neurofilament light, middle and heavy chains (NF-L, NF-M and NF-H). As with other members of the intermediate filament family, neurofilament proteins share a common structural organization that comprises a central α-helical rod domain that is flanked by N-terminal head and C-terminal tail domains (9,10). The central rod domains facilitate the formation of coiled-coil oligomers that can then assemble into filaments of 10 nm diameter; the N-terminal head domains are believed to regulate the assembly properties of the filament, and the C-terminal tail domains of NF-M and NF-H (which are longer than that of NF-L) form side-arms that project from the filament and appear to form interconnections between neurofilaments and other axoplasmic organelles (11–14).

The mutations in NF-L that are associated with CMT involve a two-base conversion at codon 8 that results in a proline-to-arginine substitution and a single conversion at codon 333 that substitutes proline for glutamine (7,8). Codon 8 resides within the head domain, whereas codon 333 is situated in coil 2B of the central rod domain of NF-L. Both Pro8 and Gln333 are highly conserved in mammals and *Xenopus*, which suggests that they are structurally and/or functionally important. However, the effects that these different CMT mutations have on neurofilament assembly and architecture are not known. Here, we demonstrate that both CMT NF-L mutant proteins disrupt neurofilament assembly and axonal transport.

## RESULTS

We initially studied the effects of the NF-L Pro8Arg and Gln333Pro mutations (NF-L$^{Pro8Arg}$ and NF-L$^{Gln333Pro}$) on neurofilament assembly in transfected SW13− cells. These cells do not express endogenous intermediate filament proteins

*To whom correspondence should be addressed at: Department of Neuroscience, PO Box P037, The Institute of Psychiatry, Kings College London, De Crespigny Park, Denmark Hill. London SE5 8AF, UK. Tel: +44 2078480393; Fax: +44 2077080017; Email: chris.miller@iop.kcl.ac.uk
†Present address:
Academic Neurology Unit, Medical School, University of Sheffield, Sheffield S10 2RX, UK.

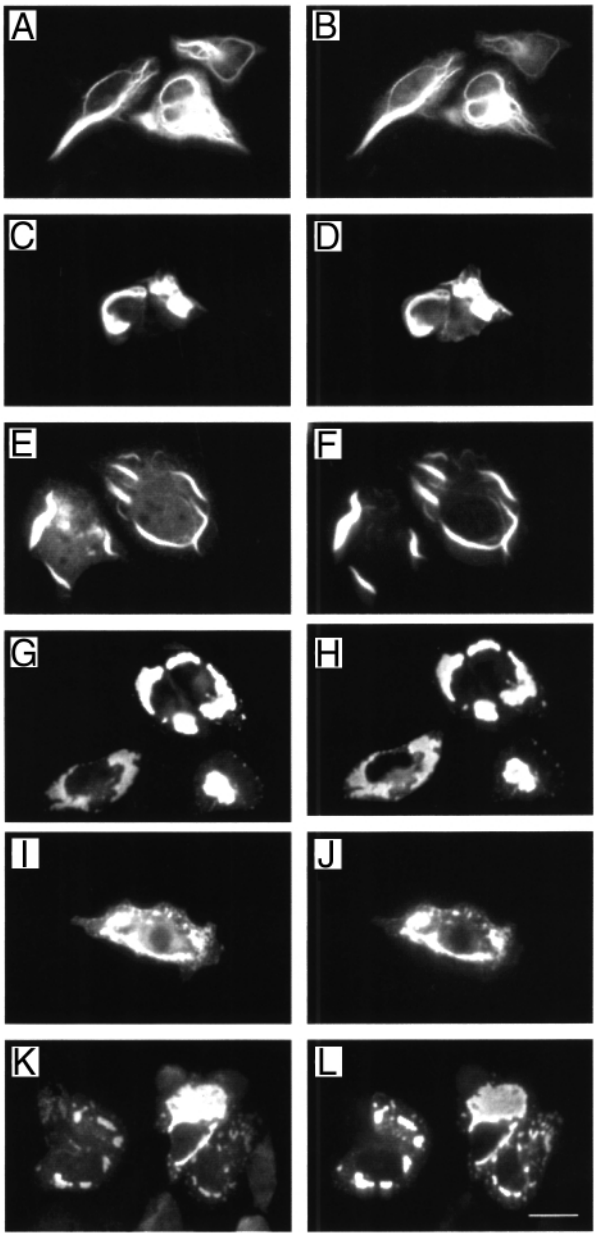


**Figure 1.** Assembly properties of human and rat NF-L$^{Pro8Arg}$ and NF-L$^{Gln333Pro}$ in SW13− cells. Cells were co-transfected with rat NF-M and NF-H, and human NF-L (**A** and **B**) human NF-L$^{Pro8Arg}$ (**C**–**F**) human NF-L$^{Gln333Pro}$ (**G** and **H**) rat NF-L$^{Pro8Arg}$ (**I** and **J**) or rat NF-L$^{Gln333Pro}$ (**K** and **L**). (A), (C), (E), (G), (I) and (K) show NF-L labelled with NA1214; (B), (D), (F), (H), (J) and (L) are labelled for NF-M/NF-H using antibody SMI32. Scale bar = 25 μm.

and so have been widely used to investigate neurofilament assembly properties (15–18). Transfection of human wild-type NF-L with NF-M and NF-H induced the formation of typical intermediate filament networks (Fig. 1A and B). However, transfection of either NF-L$^{Pro8Arg}$ or NF-L$^{Gln333Pro}$ with NF-M and NF-H disrupted these networks and led to the formation of abnormal structures containing all three proteins (Fig. 1C–H). These varied in appearance, with both smaller, punctate bodies and larger aggregates being discernible; flame-shaped structures were often seen with NF-L$^{Pro8Arg}$ (Fig. 1E and F).

There is evidence that human NF-L displays different assembly properties to rodent NF-L in SW13− cells (19). Since Pro8 and Gln333 are highly conserved, we created rat CMT NF-L$^{Pro8Arg}$ and NF-L$^{Gln333Pro}$ mutants and studied their assembly properties in SW13− cells. However, these rat CMT mutants also disrupted neurofilament assembly in a similar manner to the human mutants (Fig. 1I–L).

We next investigated the effects of the CMT mutations on neurofilament assembly *in vivo* by transfection of the mutants into rat cortical neurones. To distinguish transfected from endogenous NF-L, we utilized the human NF-L clones and detected these with a human-specific NF-L antibody. Transfected human wild-type NF-L localized to cell bodies, axons and dendrites, and higher-magnification images revealed that it co-assembled with endogenous NF-M into filaments (Fig. 2A–C). These findings are in agreement with previous studies of neurofilaments transfected into rat neurones (17,20–22). However, transfection of either NF-L$^{Pro8Arg}$ or NF-L$^{Gln333Pro}$ both disrupted neurofilament architecture. In cells transfected with the CMT mutants, transfected NF-L co-localized with endogenous NF-M (although occasional images indicated the presence of some NF-L-only-containing structures), but these mutant neurofilament proteins accumulated in the cell body or the cell body and proximal regions of neurites; the CMT mutants were rarely seen in more distal regions of axons. Abnormal neurofilament aggregates, reminiscent of those seen in the SW13− cells, were also commonly seen in cell bodies, and these were particularly noticeable in cells expressing higher levels of transfected CMT NF-L (as judged by intensity of fluorescence) (Figure 2D–G). Such aggregates were never seen in cells expressing wild-type NF-L.

Cells that are affected in CMT include sensory neurones in the dorsal root ganglion (DRG). We therefore studied the effect of expressing wild-type and CMT mutant NF-Ls in cultured DRG neurones. Transfected wild-type NF-L localized to cell bodies and axons in a similar fashion to that seen in cortical neurones (Figure 3A and B). However, both NF-L$^{Pro8Arg}$ and NF-L$^{Gln333Pro}$ again accumulated in cell bodies and proximal axons. In the DRG neurones, the cell body accumulations generally appeared as a single aggregate (Figure 3C–F).

To gain some insight into the polymeric form of NF-L$^{Pro8Arg}$ and NF-L$^{Gln333Pro}$, we prepared Triton X-100-insoluble and -soluble fractions from SW13− cells co-transfected with NF-M and NF-H and wild-type NF-L, NF-L$^{Pro8Arg}$ or NF-L$^{Gln333Pro}$, and analysed the distribution of the individual neurofilament proteins. Neurofilament proteins that are assembled into intermediate filaments are present in the Triton X-100-insoluble fraction of such preparations. In these experiments, NF-L$^{Pro8Arg}$ and NF-L$^{Gln333Pro}$ fractionated to the Triton X-100-insoluble component at both 15 000*g* (average) and 100 000*g* (average) (Fig. 4). The pelleting of the mutant NF-Ls suggests that they are assembled into a polymeric form of higher order than the tetrameric stage. Thus, both CMT mutant proteins disrupt normal neurofilament assembly in SW13− cells and neurones, but their co-localization with NF-M/NF-H and presence in a Triton X-100-insoluble fraction indicate that this does not preclude co-assembly with other neurofilament proteins.

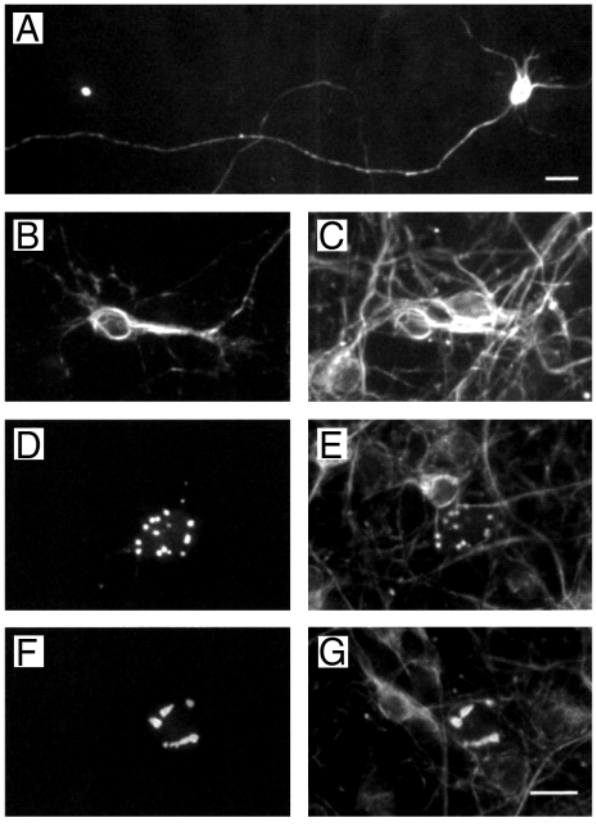


**Figure 2.** Assembly properties of NF-L$^{Pro8Arg}$ and NF-L$^{Gln333Pro}$ in rat cortical neurones. Cells were transfected with human clones for wild-type NF-L (**A**–**C**) NF-L$^{Pro8Arg}$ (**D** and **E**) or NF-L$^{Gln333Pro}$ (**F** and **G**). (A), (B), (D) and (F) are labelled for NF-L using human-specific monoclonal antibody anti-NF70; (C), (E) and (G) are labelled for NF-M using rabbit antibody NF-M-Cterm. Scale bars = 25 μm.

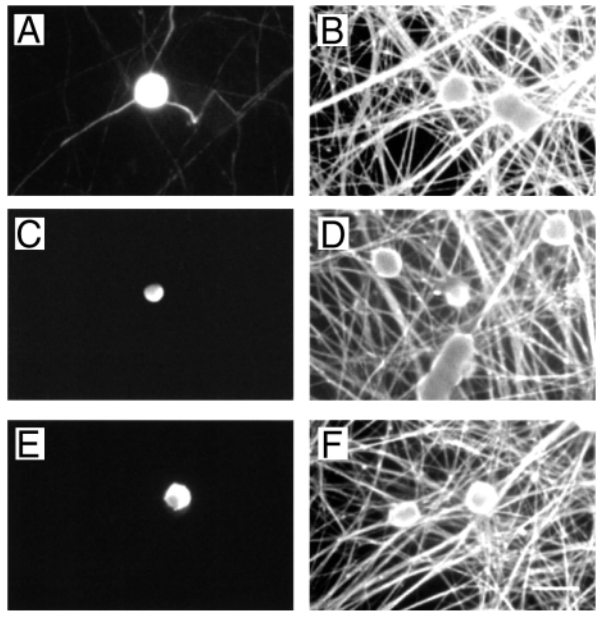


**Figure 3.** Assembly and transport properties of NF-L$^{Pro8Arg}$ and NF-L$^{Gln333Pro}$ in rat DRG neurones. Cells were transfected with human clones for wild-type NF-L (**A** and **B**) NF-L$^{Pro8Arg}$ (**C** and **D**) or NF-L$^{Gln333Pro}$ (**E** and **F**). (A), (C) and (E) are labelled for NF-L using human-specific monoclonal antibody anti-NF70; (B), (D) and (F) are labelled for NF-M using rabbit antibody NF-M-Cterm. Scale bar = 40 μm.

Neurofilament proteins are synthesized in cell bodies and then transported into and through axons (23–26). The restriction of NF-L$^{Pro8Arg}$ and NF-L$^{Gln333Pro}$ to cell bodies and proximal regions of axons in the transfected cortical and DRG neurones suggests that the mutants somehow disrupt axonal transport of neurofilaments. We therefore analysed the effects of the two CMT mutants on axonal transport of neurofilaments using a previously described assay (17). This assay involves monitoring movement of enhanced green fluorescent protein (EGFP)-tagged NF-M in transfected cortical neurones by fixation of cells at set time points and measurement of the distance travelled by the fluorescent EGFP–NF-M front. EGFP–NF-M co-transfected with wild-type human NF-L travelled at a rate of ~80 μm/h (Fig. 5A). This is in close agreement with that previously calculated by us for cells transfected with EGFP–NF-M alone (17), and demonstrates that co-transfection with NF-L has little, if any, effect on the movement of EGFP–NF-M. However, co-transfection of either NF-L$^{Pro8Arg}$ or NF-L$^{Gln333Pro}$ significantly reduced the distance travelled by EGFP–NF-M (Fig. 5B).

In a complementary study, we also analysed the effect of the CMT mutant NF-Ls on axonal transport of mitochondria by quantifying the distribution of mitochondria in a defined segment of axons. This approach has recently been successfully used to study the effect of transfected tau on mitochondrial transport (27). To do so, we transfected DRG neurones with a marker for mitochondria (*Discosoma* red fluorescent protein fused to the mitochondrial targeting sequence from subunit V111 of human cytochrome *c* oxidase, DsRed2–Mito) (28) either alone or with human wild-type NF-L, NF-L$^{Pro8Arg}$ or NF-L$^{Gln333Pro}$. Cells transfected with DsRed2–Mito alone revealed that mitochondria were present in cell bodies and throughout the length of neurites (Fig. 6A and B) which is in agreement with other studies on the distribution of mitochondria in neurones (27). Similar images were obtained from cells co-transfected with DsRed2–Mito and wild-type NF-L (Fig. 6C and D). However, mitochondria in cells co-transfected with DsRed2–Mito and either NF-L$^{Pro8Arg}$ or NF-L$^{Gln333Pro}$ were clustered in cell bodies and proximal axons, with markedly fewer present in more distal regions of axons (Figure 6E–H). To quantify this, we counted the number of mitochondria present in a defined segment of axons, 50–100 μm from the cell body. These studies revealed that significantly fewer mitochondria were present in this region in cells co-transfected with either NF-L$^{Pro8Arg}$ or NF-L$^{Gln333Pro}$ compared with cells transfected with wild-type NF-L (Fig. 6I). Thus, the two CMT mutant neurofilament proteins inhibit axonal transport of both neurofilaments and mitochondria.

## DISCUSSION

An increasing body of evidence suggests that disruptions to neurofilament metabolism are part of the disease process in a number of neurodegenerative diseases. Two NF-L mutations have so far been described as causative for CMT2. However,

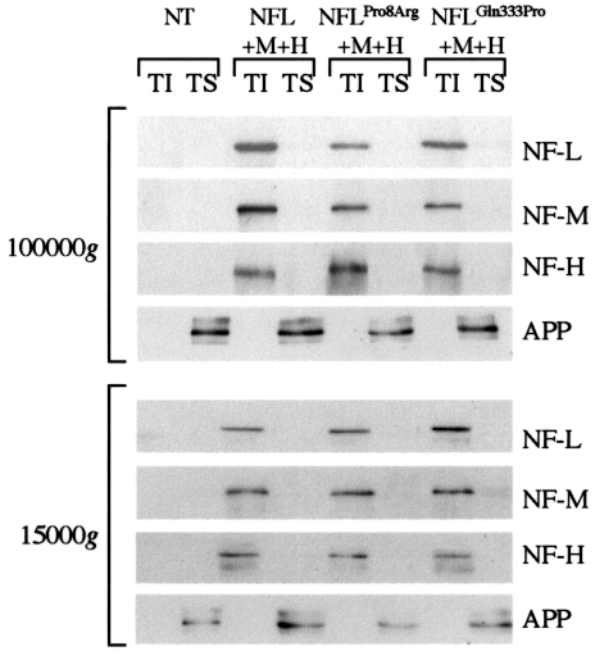


**Figure 4.** Biochemical properties of NF-L$^{Pro8Arg}$ and NF-L$^{Gln333Pro}$. Triton X-100-insoluble (TI) and -soluble (TS) fractions were prepared from SW13− cells transfected with NF-M and NF-H, and wild-type human NF-L, NF-L$^{Pro8Arg}$ or NF-L$^{Gln333Pro}$. NT are non-transfected cells. Fractions were prepared at 15 000*g* (average) and 100 000*g* (average) as indicated. Fractionation of APP to the Triton X-100-soluble component is shown as a control. Similar results were obtained using rat NF-L.

NFL mutations in several further CMT families have now been identified and probably account for ∼2% of CMT kindreds (V. Timmerman, personal communication). Aside from these NF-L CMT2 mutations, mutations in NF-H have been shown to be a risk factor for amyotrophic lateral sclerosis (ALS) (29–31), and recently a mutation in NF-M has been linked to familial Parkinson's disease (32). ln addition, accumulations of neurofilaments are a pathology of several neurodegenerative diseases including ALS, Alzheimer's disease, Parkinson's disease, dementia with Lewy bodies and diabetic neuropathy (for reviews see 26,33,34). Also, overexpression of neurofilament proteins, including peripherin, in transgenic mice can provide models of ALS (35–38), and modulating neurofilament expression alters disease progression in transgenic models of ALS caused by mutant superoxide dismutase 1 (SOD1) (39–42). Interestingly, transgenic mice expressing a mutant NF-L in which codon 394 (close to the CMT2 codon 333 mutation) is mutated from leucine to proline develop a particularly aggressive form of motor neurone disease (37). Finally, overexpression of peripherin has recently been shown to induce apoptotic death of neurones that is mediated by the proinflammatory cytokine tumour necrosis factor α (TNF-α) (43).

Disruption of axonal transport of neurofilaments is one of the earliest pathological features seen in these transgenic models of ALS (44–46), and this suggests that it is a primary pathogenic event that induces disease and not some end-stage epiphenomenon. It is thus notable that both CMT2 mutant NF-Ls disrupt axonal transport of neurofilaments.

We also demonstrate that these mutant NF-Ls perturb transport of mitochondria into and through axons, leading to their accumulation in cell bodies and proximal axons. Neurones are highly polarized cells with organelles, vesicles and other protein complexes requiring transportation to their appropriate final destinations following synthesis. The distances involved in this transport can be considerable; for example, human motor neurone axons can exceed 1 m in length. The accumulation of mitochondria in cell bodies and proximal axons strongly suggests that the supply of metabolic energy to more distal regions of axons and dendrites is impaired in CMT. This will perturb the functioning of kinesin and dynein family motors, which both require ATP, and, as such, disrupt the supply of essential axoplasmic components. It is likely that this disruption is mechanistic in neuronal cell death in CMT. Indeed, mutation of KlF1bβ (a molecular motor protein) has been shown to cause another form of type 2 CMT (47), and this further implicates axonal transport in the disease process.

Our results presented here, showing that two NF-L mutations linked to CMT disrupt neurofilament assembly and axonal transport, demonstrate that defective neurofilament metabolism can induce neurological disease.

## MATERIALS AND METHODS

All of the experiments described in the Results section were performed at least three times with similar results.

### Plasmids

Expression plasmids for human and rat neurofilaments including EGFP–NF-M were as previously described (17,48). Mutants were prepared using Stratagene Quickchange or Chameleon kits according to the manufacturers' instructions Mutagenic oligonucleotides were 5′-GTTCCTTCAGCTACG-AGAGGTACTACTCGACCTCC-3′ and 5′-GGAGGTCGAGT-AGTACCTCTCGTAGCTGAAGGAAC-3′ (human NF-L$^{Pro8Arg}$); 5′-GAAGCGCTGGAGAAGCCGCTGCAGGAGCTGGAGG-3′ and 5′-CCTCCAGCTCCTGCAGCGGCTTCTCCAGCGCTTC-3′ (human NF-L$^{Gln333Pro}$); 5′-GTTCGTTCAGCTACGAGAGGT-ACTTTTCGACCTCC-3′ (rat NF-L$^{Pro8Arg}$); 5′-GAAGCTCTA-GAGAAGCCGCTGCAGGAGCTGGAG-3′ (rat NF-L$^{Gln333Pro}$). Mitochondria were visualized by transfection with the vector pDsRed2–Mito (Clontech).

### Cell culture, transfection and immunofluorescence microscopy

SW13− cells were grown in DMEM containing 10% (v/v) fetal bovine serum (FBS) supplemented with 2 mM glutamine, 100 IU/ml penicillin and 100 μg/ml streptomycin (Invitrogen) and transfected using Lipofectamine 2000 (Invitrogen), essentially according to the manufacturer's instructions. For immunofluorescence studies, cells were cultured in 12-well plates (Falcon) on glass coverslips. Primary cortical neurones were obtained from E18 rat embryos and cultured on glass coverslips coated with poly-D-lysine in 12-well plates in Neurobasal medium and B27 supplement (lnvitrogen) containing 100 IU/ml penicillin, 100 μg/ml streptomycin and 2 mM glutamine. Cells were cultured for 7 days, and under these conditions were

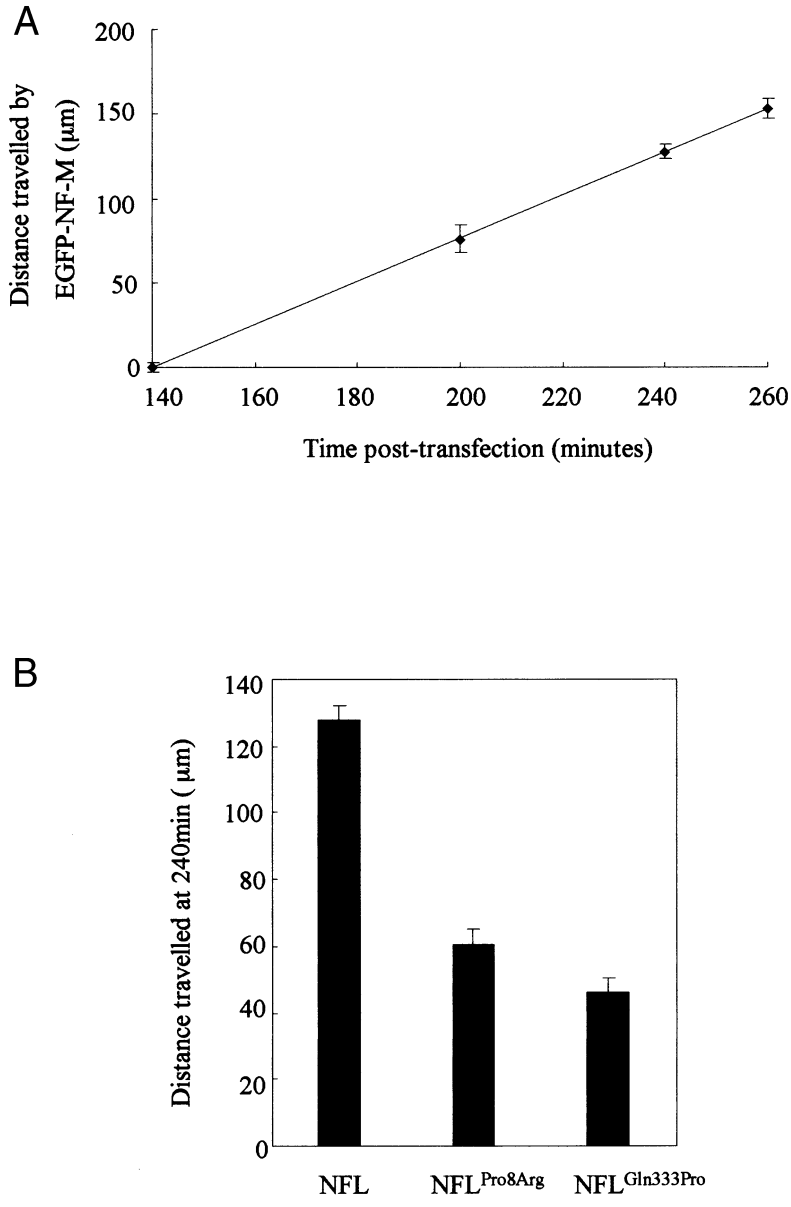


**Figure 5.** Neurofilament transport in rat cortical neurones. Cells were co-transfected with rat EGFP–NF-M and human wild-type NF-L, NF-L$^{Pro8Arg}$ or NF-L$^{Gln333Pro}$, and the distance travelled by EGFP–NF-M was then calculated. **(A)** Rate of transport of EGFP–NF-M in cells co-transfected with wild-type NF-L. **(B)** Distance travelled by EGFP–NF-M at the 240 min time point in cells co-transfected with wild-type NF-L, NF-L$^{Pro8Arg}$ or NF-L$^{Gln333Pro}$. One-way ANOVA tests revealed significant differences ($P < 0.001$) in the distances travelled by EGFP–NF-M between wild-type NF-L and NF-L$^{Pro8Arg}$ or NF-L$^{Gln333Pro}$ co-transfected cells. Error bars are SEM.

almost exclusively neurones, as previously described by us and others (17,49). Cortical neurones were transfected using a Promega calcium phosphate Profection kit essentially as previously described (17,49,50). Cells were transfected with plasmid DNA prepared using an EndoFree plasmid kit (Qiagen). DRG neurones were obtained from E15 rat embryos and grown on poly-D-lysine- and laminin - coated coverslips in Neurobasal media and B27 supplement containing 100 IU/ml penicillin, 100 μg/ml streptomycin, 2 mM glutamine and 0.1 μg/ml nerve growth factor (Sigma). Cells were transfected using Lipofectamine 2000. Briefly, media from 7-day-old neurones grown in 12-well dishes was removed and replaced with 0.5 ml Optimem (Invitrogen) containing 2 μg plasmid DNA and 3.5 μl Lipofectamine 2000. Cells were incubated for 4 h, and the Optimem was then removed and replaced with the conditioned Neurobasal/B27 medium.

Cells were fixed and processed for immunofluorescence microscopy 40 h post transfection. Briefly, cells were fixed in 4% (w/v) paraformaldehyde in PBS for 20 min, permeabilized in 0.1% (w/v) Triton X-100 in PBS for 10 min, blocked with 5% (v/v) FBS/0.1% (w/v) Tween-20 in PBS for 1 h, and then probed with primary antibodies diluted in blocking solution.

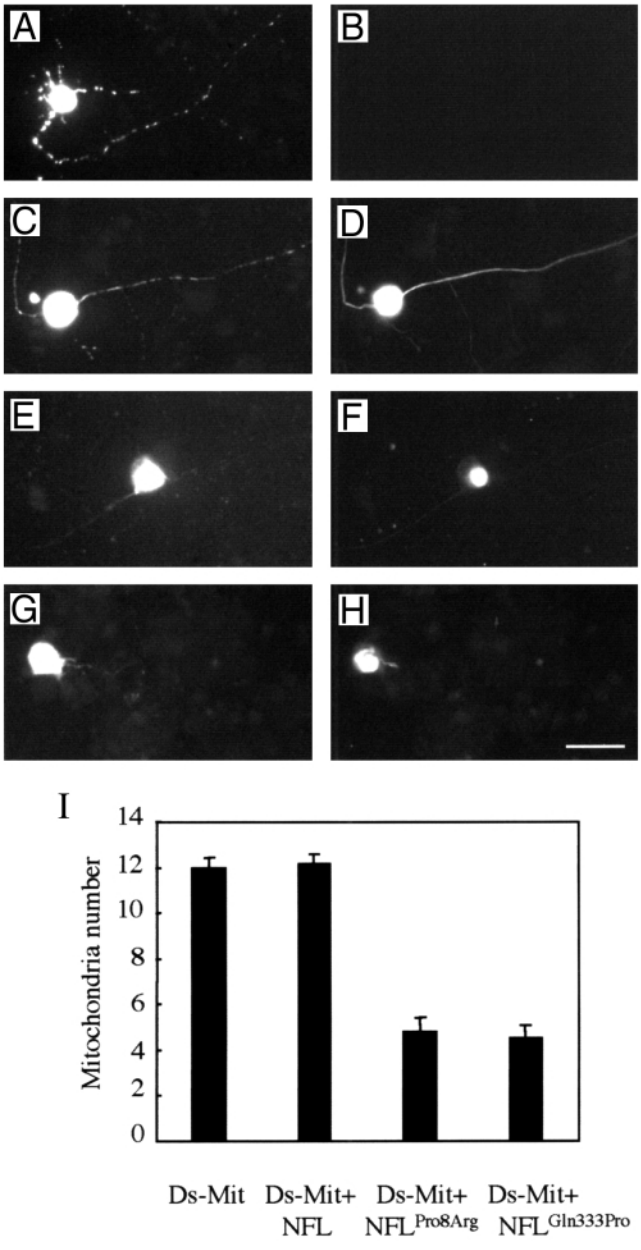


**Figure 6.** Aberrant localization of mitochondria in DRG neurones expressing NF-L$^{Pro8Arg}$ and NF-L$^{Gln333Pro}$. Cells were transfected with DsRed2–Mito (Ds-Mit) either alone (**A** and **B**) or with human clones for wild-type NF-L (**C** and **D**), NF-L$^{Pro8Arg}$ (**E** and **F**) or NF-L$^{Gln333Pro}$ (**G** and **H**). (A), (C), (E) and (G) show DsRed2–Mito fluorescence; (B), (D), (F) and (H) show human NF-L. Scale bar = 40 µm. (I) Quantification of mitochondria distribution in a segment of axon 50 µm in length beginning 50 µm from the cell body. Expression of wild-type NF-L has no effect on the distribution of mitochondria, but expression of either NF-L$^{Pro8Arg}$ or NF-L$^{Gln333Pro}$ significantly (one-way ANOVA $P < 0.001$) reduces mitochondria numbers in this segment. Error bars are SEM.

NF-L was detected using antibody NA1214 (Affiniti) and human-specific monoclonal antibody anti-NF70 (Chemicon). NF-M/NF-H were detected using antibody SMI32 (Sternberger Monoclonals Inc.) and NF-M using rabbit antibody NF-M-Cterm (Chemicon). Primary antibodies were then detected using goat anti-mouse or goat anti-rabbit immunoglobulins coupled to Oregon Green or Texas Red (Molecular Probes) and the samples were mounted in Vectashield (Vector Labs). Cells were examined using a Zeiss Axioskop microscope and images were collected via a CCD camera (Princeton Instruments).

### Analyses of bulk neurofilament transport in rat cortical neurones

Bulk transport of neurofilaments was analysed using a previously described assay (17). Briefly, neurones cultured for 7 days were co-transfected with EGFP–NF-M and human wild-type NF-L, NF-L$^{Pro8Arg}$ or NF-L$^{Gln333Pro}$, and the cells were then fixed in 4% paraformaldehyde as described above 140, 200, 240 and 260 minutes post transfection. Cells were immunostained for human NF-L using antibody anti-NF70 in order to confirm co-expression, and images of EGFP–NF-M transfected cells were then collected (≥30 images per time point) via a CCD camera. Measurements of the distance travelled by EGFP–NF-M were calculated using Metamorph image analysis software. In these studies, measurements of the distance travelled by EGFP–NF-M were taken from the cell body to the front of the fluorescent signal and were of the longest distances in each neurone. The fluorescent front was taken as the most distal point at which fluorescence above background was detected. For neurites that exhibited branching, measurements were of the major neurite as determined by length and brightness of fluorescence. Since we measured the distance travelled by EGFP–NF-M for <300 µm from the cell body, and since the average length of the major neurites in the transfected cortical neurones >700 µm, this assay of neurofilament movement is of transport within neurites and is not a reflection of EGFP–NF-M in neurite terminals and neurite growth rates [for further discussion on this point see (17)]. To simplify presentation of the data and to facilitate comparisons between different experiments, the distance travelled by EGFP–NF-M at the first (140 min) time point is adjusted to zero. Statistical analyses of neurofilament transport were performed using one-way ANOVA tests.

### Quantification of mitochondria in rat DRG neurones

For analyses of mitochondria distribution, DRG neurones were transfected with the mitochondrial marker DsRed2–Mito either alone or in co-transfections with human wild-type NF-L, NF-L$^{Pro8Arg}$ or NF-L$^{Gln333Pro}$, and were fixed for analyses 40 h later. Following immunostaining for human NF-L with anti-NF-70 and Oregon Green-conjugated anti-mouse immunoglobulins, mitochondria were visualized using the *Discosoma* red fluorescent protein. Mitochondrial distribution was analysed using a modification of the method previously described for such analyses in N2a cells (27). Briefly, images of transfected cells (≥30 cells per transfection) were captured, and a defined area of axon, 50 µm in length beginning 50 µm from the cell body was circumscribed manually using Metamorph. The number of mitochondria in this segment of axon were then visualized and counted using the threshold function of Metamorph. Statistical analyses of mitochondria distribution were performed using one-way ANOVA tests.

### Neurofilament preparation, SDS–PAGE and immunoblotting

Triton X-100-insoluble and -soluble fractions were prepared from SW13− cells transfected with NF-L, NF-M and NF-H. To do so, cells were scraped into PBS containing 0.5% Triton X-100, 0.6 M KCl, 5 mM EDTA, 5 mM EGTA, 40 µg/ml leupeptin (Sigma) and Complete protease inhibitor cocktail (Roche). The cells were then homogenized using a motorized homogeniser and the sample was spun at either 15 000*g* (average) for 15 min or 100 000*g* (average) for 30 min. Supernatants and pellets were separated and prepared for SDS–PAGE by addition of SDS–PAGE sample buffer and heating in a boiling water bath. Equal proportions of these fractions, each representing the same number of cells, were analysed by SDS–PAGE and immunoblotting. NF-L, NF-M and NF-H were detected using antibodies NA1214, NA1216 and NA1211 (Affiniti) respectively. The amyloid precursor protein (APP), a membrane-associated protein that is soluble in Triton X-100, was detected using antibody 22C11 (Roche Molecular Biochemicals), and was used as a control.

## ACKNOWLEDGEMENTS

This work was supported by grants from the Medical Research Council, the UK Motor Neurone Disease Association and the Wellcome Trust. We thank Ron Liem (New York) and Jean-Pierre Julien (Montreal) for kind gifts of neurofilament DNA clones. We also thank Vincent Timmerman, University of Antwerp, for communicating his unpublished results.

## REFERENCES

1. Reilly, M.M. (2000) Classification of the hereditary motor and sensory neuropathies. *Curr. Opin. Neurol.*, **13**, 561–564.
2. Young, P. and Suter, U. (2001) Disease mechanisms and potential therapeutic strategies in Charcot–Marie–Tooth disease. *Brain Res. Rev.*, **36**, 213–221.
3. Bennett, C.L. and Chance, P.F. (2001) Molecular pathogenesis of hereditary motor, sensory and autonomic neuropathies. *Curr. Opin. Neurol.*, **14**, 621–627.
4. Baxter, R.V., Othmane, K.B., Rochelle, J.M., Stajich, J.E., Hulette, C., Dew-Knight, S., Hentati, F., Hamida, M.B., Bel, S., Stenger, J.E. *et al.* (2002) Ganglioside-induced differentiation-associated protein-1 is mutant in Charcot–Marie–Tooth disease 4A/8q21. *Nat. Genet.*, **30**, 21–22.
5. Cuesta, A., Pedrola, L., Sevilla, T., Garcia-Planells, J., Chumillas, M.J., Mayordomo, F., LeGuern, E., Marin, I., Vilchez, J.J. and Palau, F. (2002) The gene encoding ganglioside-induced differentiation-associated protein 1 is mutated in Charcot–Marie–Tooth type 4A disease. *Nat. Genet.*, **30**, 22–25.
6. Boerkoel, C.F., Takashima, H., Garcia, C.A., Olney, R.K., Johnson, J., Berry, K., Russo, P., Kennedy, S., Teebi, A.S., Scavina, M. *et al.* (2002) Charcot–Marie–Tooth disease and related neuropathies: Mutation distribution and genotype–phenotype correlation. *Ann. Neurol.*, **51**, 190–201.
7. Mersiyanova, I.V., Perepelov, A.V., Polyakov, A.V., Sitnikov, V.F., Dadali, E.L., Oparin, R.B., Petrin, A.N. and Evgrafov, O.V. (2000) A new variant of Charcot–Marie–Tooth disease type 2 is probably the result of a mutation in the neurofilament-light gene. *Am. J. Hum. Genet.*, **67**, 37–46.
8. De Jonghe, P., Mersivanova, I., Nelis, E., Del Favero, J., Martin, J.J., Van Broeckhoven, C., Evgrafov, O.C. and Timmerman, V. (2001) Further evidence that neurofilament light chain gene mutations can cause Charcot–Marie–Tooth disease type 2E. *Ann. Neurol.*, **49**, 245–249.
9. Lee, M.K. and Cleveland, D.W. (1996) Neuronal intermediate filaments. *Annu. Rev. Neurosci.*, **19**, 187–217.
10. Grant, P. and Pant, H.C. (2000) Neurofilament protein synthesis and phosphorylation. *J. Neurocytol.*, **29**, 843–872.
11. Gill, S.R., Wong, P.C., Monteiro, M.J. and Cleveland, D.C. (1990) Assembly properties of dominant and recessive mutations in the small mouse neurofilament (NF-L) subunit. *J. Cell Biol.*, **111**, 2005–2019.
12. Ching, G.Y. and Liem, R.K.H. (1999) Analysis of the roles of the head domains of type IV rat neuronal intermediate filament proteins in filament assembly using domain-swapped chimeric proteins. *J. Cell Sci.*, **112**, 2233–2240.
13. Nakagawa, T., Chen, J., Zhang, Z., Kanai, Y. and Hirokawa, N. (1995) Two distinct functions of the carboxyl-terminal tail domain of NF-M upon neurofilament assembly: cross-bridge formation and the longitudinal elongation of filaments. *J. Cell Biol.*, **129**, 411–429.
14. Chen, J.G., Nakata, T., Zhang, Z.Z. and Hirokawa, N. (2000) The C-terminal tail domain of neurofilament protein-H (NF-H) forms the crossbridges and regulates neurofilament bundle formation. *J. Cell Sci.*, **113**, 3861–3869.
15. Ching, G.Y. and Liem, R.K. (1993) Assembly of type IV neuronal intermediate filaments in nonneuronal cells in the absence of preexisting cytoplasmic intermediate filaments. *J. Cell Biol.*, **122**, 1323–1335.
16. Lee, M.K., Xu, Z., Wong, P.C. and Cleveland, D.W. (1993) Neurofilaments are obligate heteropolymers *in vivo*. *J. Cell Biol.*, **122**, 1337–1350.
17. Ackerley, S., Grierson, A.J., Brownlees, J., Thornhill, P., Anderton, B H., Leigh, P.N., Shaw, C.E. and Miller, C.C.J. (2000) Glutamate slows axonal transport of neurofilaments in transfected neurons. *J. Cell Biol.*, **150**, 165–175.
18. Wang, L. and Brown, A. (2001) Rapid intermittent movement of axonal neurofilaments observed by fluorescence photobleaching. *Mol. Biol. Cell*, **12**, 3257–3267.
19. Carter, J., Gragerov, A., Konvicka, K., Elder, G., Weinstein, H. and Lazzarini, R.A. (1998) Neurofilament (NF) assembly; divergent characteristics of human and rodent NF-L subunits. *J. Biol. Chem.*, **273**, 5101–5108.
20. Yabe, J.T., Pimenta, A. and Shea, T.B. (1999) Kinesin-mediated transport of neurofilament protein oligomers in growing axons. *J. Cell Sci.*, **112**, 3799–3814.
21. Wang, L., Ho, C.-I., Sun, D., Liem, R.K.H. and Brown, A. (2000) Rapid movement of axonal neurofilaments interrupted by prolonged pauses. *Nat. Cell Biol.*, **2**, 137–141.
22. Roy, S., Coffee, P., Smith, G., Liem, R.K.H., Brady, S.T. and Black, M.M. (2000) Neurofilaments are transported rapidly but intermittently in axons: Implications for slow axonal transport. *J. Neurosci.*, **20**, 6849–6861.
23. Brown, A. (2000) Slow axonal transport: stop and go traffic in the axon. *Nat. Rev. Mol. Cell Biol.*, **1**, 153–156.
24. Shea, T.B. and Flanagan, L.A. (2001) Kinesin, dynein and neurofilament transport. *Trends Neurosci.*, **24**, 644–648.
25. Shah, J.V. and Cleveland, D.W. (2002) Slow axonal transport: fast motors in the slow lane. *Curr. Opin. Cell Biol.*, **14**, 58–62.
26. Miller, C.C.J., Ackerley, S., Brownlees, J., Grierson, A.J., Jacobsen, N.J.O. and Thornhill, P. (2002) Axonal transport of neurofilaments in normal and disease states. *Cell. Mol. Life Sci.*, **59**, 323–330.
27. Stamer, K., Vogel, R., Thies, E., Mandelkow, E. and Mandelkow, E.-M. (2002) Tau blocks traffic of organelles, neurofilaments, and APP vesicles in neurons and enhances oxidative stress. *J. Cell Biol.*, **156**, 1051–1063.
28. Rizzuto, R., Brini, M., Pizzo, P., Murgia, M. and Pozzan, T. (1995) Chimeric green fluorescent protein as a tool for visualizing subcellular organelles in living cells. *Curr. Biol.*, **5**, 635–642.
29. Figlewicz, D.A., Krizus, A., Martinoli, M.G., Meininger, V., Dib, M., Rouleau, G.A. and Julien, J.-P. (1994) Variants of the heavy neurofilament subunit are associated with the development of amyotrophic lateral sclerosis. *Hum. Mol. Genet.*, **3**, 1757–1761.
30. Tomkins, J., Usher, P., Slade, J.Y., Ince, P.G., Curtis, A., Bushby, K. and Shaw, P.J. (1998) Novel insertion in the KSP region of the neurofilament heavy gene in amyotrophic lateral sclerosis (ALS). *Neuroreport*, **9**, 3967–3970.
31. AI-Chalabi, A., Anderson, P.M., Nilsson, P., Chioza, B., Andersson, J.L., Russ, C.R., Shaw, C.E., Powell, J.F. and Leigh, P.N. (1999) Deletions of the heavy neurofilament subunit tail in amyotrophic lateral sclerosis. *Hum. Mol. Genet*, **8**, 157–164.
32. Lavedan, C., Buchholtz, S., Nussbaum, R.L., Albin, R.L and Polymeropoulos, M.H. (2002) A mutation in the human neurofilament

M gene in Parkinson's disease that suggests a role for the cytoskeleton in neuronal degeneration. *Neurosci. Lett.*, **322**, 57–61.
33. Julien, J.P. (1999) Neurofilament functions in health and disease. *Curr. Opin. Neurobiol.*, **9**, 554–560.
34. Cleveland, D.W. and Rothstein, J.D. (2001) From Charcot to Lou Gehrig: deciphering selective motor neuron death in ALS. *Nat. Rev. Neurosci.*, **2**, 806–819.
35. Cote, F., Collard, J.-F. and Julien, J.-P. (1993) Progressive neuronopathy in transgenic mice expressing the human neurofilament heavy gene: a mouse model of amyotrophic lateral sclerosis. *Cell*, **73**, 35–46.
36. Xu, Z., Cork, L.C., Griffin, J.W. and Cleveland, D.W. (1993) Increased expression of neurofilament subunit NF-L produces morphological alterations that resemble the pathology of human motor neuron disease. *Cell*, **73**, 23–33.
37. Lee, M.K., Marszalek, J.R. and Cleveland, D.W. (1994) A mutant neurofilament subunit causes massive, selective motor neuron death: Implications for the pathogenesis of human motor neuron disease. *Neuron*, **13**, 975–988.
38. Beaulieu, J.M., Nguyen, M.D. and Julien, J.P. (1999) Late onset death of motor neurons in mice overexpressing wild-type peripherin. *J. Cell Biol.*, **147**, 531–544.
39. Couillard-Després, S., Zhu, Q.Z., Wong, P.C., Price, D.L., Cleveland, D.W. and Julien, J.P. (1998) Protective effect of neurofilament heavy gene overexpression in motor neuron disease induced by mutant superoxide dismutase. *Proc. Natl Acad. Sci. USA*, **95**, 9626–9630.
40. Williamson, T.L., Bruijn, L.I., Zhu, Q.Z., Anderson, K.L., Anderson, S.D., Julien, J.P. and Cleveland, D.W. (1998) Absence of neurofilaments reduces the selective vulnerability of motor neurons and slows disease caused by a familial amyotrophic lateral sclerosis-linked superoxide dismutase 1 mutant *Proc. Natl Acad. Sci. USA*, **95**, 9631–9636.
41. Kong J.M. and Xu, Z.S. (2000) Overexpression of neurofilament subunit NF-L and NF-H extends survival of a mouse model for amyotrophic lateral sclerosis. *Neurosci. Lett.*, **281**, 72–74.
42. Nguyen, M.D., Larivière, R.C. and Julien, J.P. (2001) Deregulation of Cdk5 in a mouse model of ALS: toxicity alleviated by perikaryal neurofilament inclusions. *Neuron*, **30**, 135–147.
43. Robertson, J., Beaulieu, J.M., Doroudchi, M.M., Durham, H.D., Julien, J.P. and Mushynski, W.E. (2001) Apoptotic death of neurons exhibiting peripherin aggregates is mediated by the proinflammatory cytokine TNFα. *J. Cell Biol.*, **155**, 217–226.
44. Collard, J.-F., Cote, F. and Julien, J.-P. (1995) Defective axonal transport in a transgenic mouse model of amyotrophic lateral sclerosis. *Nature*, **375**, 61–64.
45. Zhang, P., Tu, P.-h., Abtahian, F., Trojanowski, J.Q. and Lee, V.M.-Y. (1997) Neurofilaments and orthograde transport are reduced in ventral root axons of transgenic mice that express human SOD1 with a G93A mutation. *J. Cell. Biol.*, **139**, 1307–1315.
46. Williamson, T.L. and Cleveland, D.W. (1999) Slowing of axonal transport is a very early event in the toxicity of ALS-linked SOD1 mutants to motor neurons. *Nat. Neurosci.*, **2**, 50–56.
47. Zhao, C., Takita, J., Tanaka, Y., Setou, M., Nakagawa, T., Takeda, S., Yang, H.W., Terada, S., Nakata, T., Takei, Y. *et al.* (2001) Charcot–Marie–Tooth disease type 2a caused by mutation in a microtubule motor kif1bβ. *Cell*, **105**, 587–597.
48. Gibb, B.J.M., Robertson, J. and Miller, C.C.J. (1996) Assembly properties of neurofilament light chain $Ser^{55}$ mutants in transfected mammalian cells. *J. Neurochem.*, **66**, 1306–1311.
49. Nikolic, M., Dudek, H., Kwon, Y.T., Ramos, Y.F.M. and Tsai, L.H. (1996) The cdk5/p35 kinase is essential for neurite outgrowth during neuronal differentiation. *Genes Dev.*, **10**, 816–825.
50. Xia, Z.G., Dudek, H., Miranti, C.K. and Greenberg, M.E. (1996) Calcium influx via the NMDA receptor induces immediate-early gene-transcription by a MAP kinase/ERK-dependent mechanism. *J. Neurosci.*, **16**, 5425–5436.